Nonlinearity and image persistence of P-20 phosphor-based intensified photodiode array detectors used in CARS spectroscopy
Snelling, D. R.; Smallwood, G. J.; Sawchuk, R. A.

Publisher’s version / Version de l'éditeur:

Applied Optics, 28, 15, pp. 3226-3232, 1989

Nonlinearity and image persistence of P-20 phosphor-based intensified photodiode array detectors used in CARS spectroscopy

D. R. Snelling, G. J. Smallwood, and R. A. Sawchuk

Several self-scanning photodiode arrays (IPDA) used for CARS spectroscopy are shown to exhibit a greater image persistence than has generally been realized, and to exhibit a falloff in sensitivity that is logarithmic with decreasing output signal. These effects are attributed to the P-20 phosphor based intensifiers used in the IPDAs and are probably generic to all such detectors. A strategy for minimizing the image persistence in CARS spectroscopy is presented. A prototype detector incorporating a much faster rare earth phosphor is evaluated and shown to be more suited to single pulse CARS measurements in turbulent combustion than the IPDAs incorporating P-20 phosphors.

I. Introduction

Single-pulse, broadband coherent anti-Stokes Raman spectroscopy (CARS) has become an important diagnostic technique, particularly for combustion measurements of temperature and species concentration. The single pulse (10 ns) capability is crucial for the study of turbulent combustion environments such as gas turbine combustors, internal combustion engines, and turbulent flames. In order to record a single pulse the broadband CARS radiation is dispersed and detected using an optical multichannel detector.

The optical multichannel detectors (OMD) used for CARS spectroscopy are the intensified silicon intensified target (ISIT) vidicon and the intensified self-scanning silicon photodiode array (IPDA).[1] The vidicons are widely recognized to suffer from an image persistence or lag problem resulting from not all of the signal being removed by the scanning electron beam readout mechanism. This limits data acquisition to less than the 10-Hz laser repetition rate that is routinely used for CARS spectroscopy. The IPDA is generally regarded[1,2] as being free of image persistence problems (<0.1% image lag) and has been used in systems with laser repetition rates of up to 20 Hz.

During the course of an evaluation of a replacement IPDA detector we investigated the image persistence of a Princeton Instruments (PI) model IRY-1024 IPDA. The image persistence was considerably greater than 0.1% and, in reevaluating the Tracor Northern TN-6132 IPDA currently in use, we found that it also had greater image persistence than we had realized. The image persistence of these detectors was evaluated under typical CARS operating conditions and a new detector read strategy was implemented to minimize the effect.

The strategy employed for reading the IPDA in CARS experiments is usually not reported. Goss *et al.*,[3] in implementing a 10-Hz CARS system, attempted to minimize image persistence by scanning the detector 60 ms after the exposure to allow for maximum signal buildup and then performed two cleansing scans at the end of the 100-ms period to reduce the image persistence. We used essentially the same detector read pattern in our earlier work.[4,5] The detector read or scan sequentially determines the accumulated charge from each of the diodes in the array. The detector read pattern describes the timing sequence of detector reads for the 100-ms period between laser pulses.

The IPDA has an intensifier that is fiber-optically coupled to a photodiode array. The intensifier portion of the IPDA (or ISIT) consists of a photocathode, followed by a microchannel plate (MCP) intensifier for photoelectron amplification, and a phosphor screen. The electron gain of the MCP is typically 10^3–10^4 and can be varied by adjusting the applied voltage across the MCP. The electrons from the MCP are accelerated and impinge on the phosphor screen to produce photons. The overall light gain of the intensifier is typically 10,000–15,000. The phosphor is fiber-opti-

The authors are with National Research Council of Canada, Division of Mechanical Engineering, Ottawa, Ontario K1A OR6, Canada.

Received 1 March 1989.
0003-6935/89/153226-07$02.00/0.

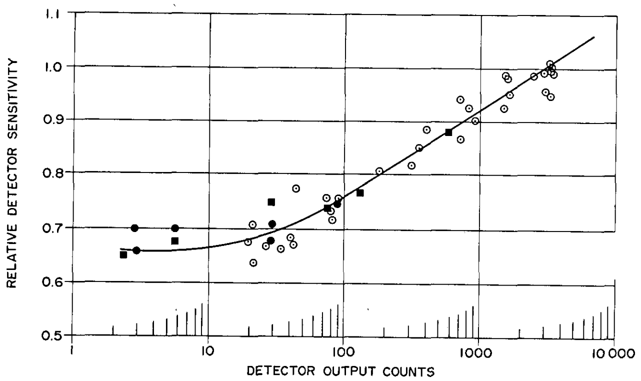

Fig. 1. Relative sensitivity of a Tracor Northern TN-6132 IPDA detector.

cally coupled to a self-scanning linear silicon photodiode array, which is cooled to reduce the dark current, and hence the thermal shot noise of the diodes. Owing to the physical contact between the intensifier and the diode array, the intensifier is also cooled to some degree.

Nonlinear behavior of the IPDA at high signal levels has been reported by several groups.[3,6,7] It is a function of radiation density[6,7] and is associated with saturation in the microchannel plate intensifier. The nonlinearity can be avoided by more uniformly illuminating the detector pixel either by adjusting the focus of the CARS spectrometer[4] or by employing a cylindrical lens to increase the CARS image size.[7]

During the course of a study on the effect of overall intensity on N_2 CARS spectral shapes we found that the IPDA detector was also exhibiting nonlinearity at low signal levels. We have subsequently investigated the nonlinearity of several P-20 phosphor-based IPDA detectors and found similar behavior, namely, a falloff in relative sensitivity that is logarithmic with decreasing detector output. A correction for this nonlinearity was incorporated into our CARS fitting computer program to assess its effect on best-fit CARS temperatures.

Both the image persistence and the low signal nonlinearity are attributable to the P-20 phosphors used in these detectors. With a typical 10-Hz CARS system the image persistence causes a signal that is 0.5–2.0% of the exposure intensity in the first read cycle following interruption of the exposure. The effect of these problems on CARS derived temperatures in turbulent combustion is discussed in a separate publication.[11]

II. Experimental

The CARS spectrometer and data acquisition system in which the IPDA detectors are used is described elsewhere.[4,6] The detector read pattern was controlled by logic circuits that allowed the timing to be adjusted to suit the experiment. Data transfer rates limited the TN-6132-based system to digitizing and storing only the first of three reads made in each 100-ms period. The PI IRY-1024-based system did not suffer from this limitation.

The source of radiation used for the nonlinearity and image persistence studies was either a room temperature N_2 CARS signal at 476 nm or frequency-doubled (2×) Nd:YAG radiation at 532 nm. The CARS signal was imaged on to the detector using a concave holographic diffraction grating.[6] For the 532-nm Nd:YAG radiation the grating was covered by a piece of white cardboard that acted as a diffuse scatterer. The scattered radiation, unlike the imaged N_2 CARS signal, uniformly illuminated each detector pixel.

The IPDA signal was compared with that obtained from a photomultiplier or silicon photodiode. A beam splitter directed part of the CARS beam (or the 2× Nd:YAG output) on to the photodetector so that its output and that of the IPDA could be monitored simultaneously.

Great care was taken to ensure that the photomultiplier was not saturating on the short duration (≈10–ns) laser pulses. Peaking capacitors were added to the final stages of the voltage divider to ensure that the voltage biasing was maintained during the pulse and the bias current was at least 20 times the average anode current. Finally, the linearity of the photomultiplier was confirmed with calibrated neutral density filters using the 532-nm 2× Nd:YAG radiation.

Both the Tracor Northern TN-6132 and the Princeton Instruments IRY-1024 used proximity-focused image intensifiers that incorporate P-20-/based phosphors. The TN-6132 used an ITT intensifier and the IRY-1024 a Varo intensifier.

Since in our earlier CARS work[4–6] the Tracor Northern TN-6132 detector cooler was operated at +2°C, we have made most of our measurements at that temperature. Because the image persistence may be a function of detector temperature we have also taken some measurements at other temperatures.

The Princeton Instruments IRY-1024 IPDA (Serial No. D 128785), which was available to us on loan, was operated at a setting of +9°C but because of limitations in the temperature control circuit[8] the actual diode array temperature was −5–8°C.

Dr. Y. Talmi of Princeton Instruments[8] has kindly provided data on the image persistence of a second IPDA as a function of temperature. Their detector was scanned continuously with the total detector read time being 33 ms. A xenon flash lamp (Stroboslave type 1539-A) was triggered synchronously with the start of a detector scan and they followed the subsequent decay of the signal.

III. Results and Discussion

A. Nonlinearity

The nonlinear behavior of one of the Tracor Northern TN-6132 IPDA detectors is shown in Fig. 1. The relative detector sensitivity (detector output in counts divided by relative light level, normalized to 1.0 at 3000 counts) was obtained by comparing the output of the IPDA with that obtained from a photomultiplier or silicon photodiode. The open circle data points in Fig. 1, which were obtained with a photomultiplier and

532-nm radiation, show that the relative detector sensitivity falls off logarithmically with decreasing IPDA output in counts to a constant value of ~0.66 at 20 counts.

We were initially surprised at this result and therefore checked additional detectors and used other verification techniques. A silicon photodiode was substituted for the photomultiplier with essentially identical results. When a room-temperature N_2 CARS signal was substituted for 2× Nd:YAG radiation very similar behavior was observed although the slope was somewhat (≈15%) less. (The difference in the slopes was just significant at the 95% confidence limit.)

We have previously reported[4] a nonlinearity at high signal levels associated with saturation in the microchannel plate intensifier when the CARS image is very much smaller than the IPDA pixel height of 2.5 mm. Although care was taken to ensure that the CARS image height was sufficient to avoid saturation, it is possible that small amounts of saturation at the higher signal levels could account for the difference in the two results since the scattered 2× Nd:YAG radiation uniformly fills the detector whereas the N_2 CARS signal is imaged on the detector.

The nonlinearity measurements using 2× Nd:YAG radiation were corroborated using single-element heavily attenuating neutral density filters. The intensifier gain (0.00–1.00) was adjustable over a 100-fold range with a 10-turn potentiometer. The solid circle data points in Fig. 1 are for an intensifier setting of 0.2 and the solid squares are for an intensifier setting of 0.83. (The photomultiplier data were recorded at an intensifier setting of 0.9. The neutral density filters were calibrated by the Photometry and Radiation Section of the Division of Physics at NRC-Canada.) The filter data are in agreement with the photomultiplier data at detector outputs of >20 counts and, in addition, show a leveling off in gain below this signal level. The results also show that the nonlinear behavior is independent of intensifier setting (microchannel plate gain).

Similar measurements were performed on a second TN-6132 and, within the error limits, identical behavior was observed. A Princeton Instruments IRY-1024 exhibited a similar logarithmic dependence of detector sensitivity which dropped from 1.0 at 13,000 counts to 0.76 at 10 counts as shown in Fig. 2.

An alternative description of the nonlinearity is given by the mathematical expression:

$$C = aI^b \tag{1}$$

where C is the detector output in counts, I is the light intensity, and typical values of the constants a and b are 0.47 and 1.09, respectively. While this equation is not identical to that implied by a logarithmic falloff in detector sensitivity (C/I) it is experimentally indistinguishable from it and is easier to use to correct experimental data at very low counts. It may also offer some clue to the source of the nonlinearity.

Results similar to these have been obtained with an EG&G/PARC system,[9] indicating that this form of

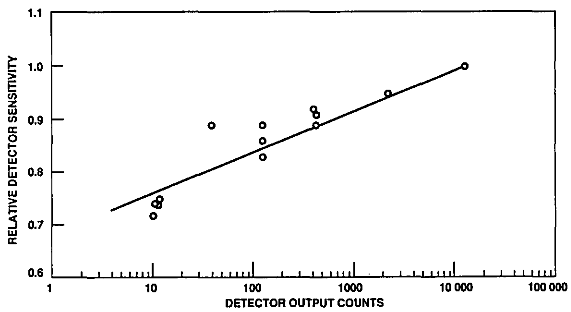

Fig. 2. Relative sensitivity of a Princeton Instruments IRY-1024 IPDA detector.

nonlinearity is widespread and is probably generic to P-20 phosphor-based IPDA detectors. We have examined a prototype Princeton Instruments IPDA incorporating a rare earth phosphor with a faster decay that does not exhibit the nonlinear behavior, further suggesting that the problem is attributable to the P-20 phosphor.[10]

The effect of IPDA nonlinearity on CARS derived temperatures is discussed in more detail in a separate publication[11] which appears in this issue. Briefly, applying a correction for detector nonlinearity results in best-fit CARS temperatures that are 40 (Fig. 2)–90 K (Fig. 1) hotter at 1600 K. This nonlinearity appears to have been neglected in earlier comparisons of CARS temperatures with temperatures obtained using other techniques, which casts doubt on the validity of those comparisons.

B. Image Persistence

The image persistence of the TN-6132 IPDA (detector temperature +2°C) shown in Fig. 3 was measured by interrupting a 10-Hz-pulsed laser exposure (2× Nd:YAG) and following the subsequent decay of the signal. The signal is expressed as a percentage of the last recorded laser pulse signal for two different detector scan patterns. Each detector read is represented by a square wave pulse and, because of data transfer rate limitations, only detector read No. 1 was digitized and stored. Reads Nos. 2 and 3 were instituted as cleansing scans to remove any accumulated signal from the IPDA before the next laser exposure occurred.

Read pattern No. 1 was the one used in our earlier work[4–6] whereas read pattern No. 2 was chosen at the end of this study to minimize image persistence. The image persistence can be detected as long as 2.8 s after the interruption of exposure with read pattern No. 1, and is much less for read pattern No. 2. For read pattern No. 2 the image persistence was also measured for detector temperatures of −2°C and +20°C. The image persistence in the first cycle following the last exposure was 0.62 ± 0.04% (−2°C) and 0.52 ± 0.04% (20°C). The change of image persistence with temperature over the range −2–+20°C is barely detectable for the TN-6132 IPDA.

The image persistence of an unintensified diode array (Fig. 3) is much less than for the intensified detec-

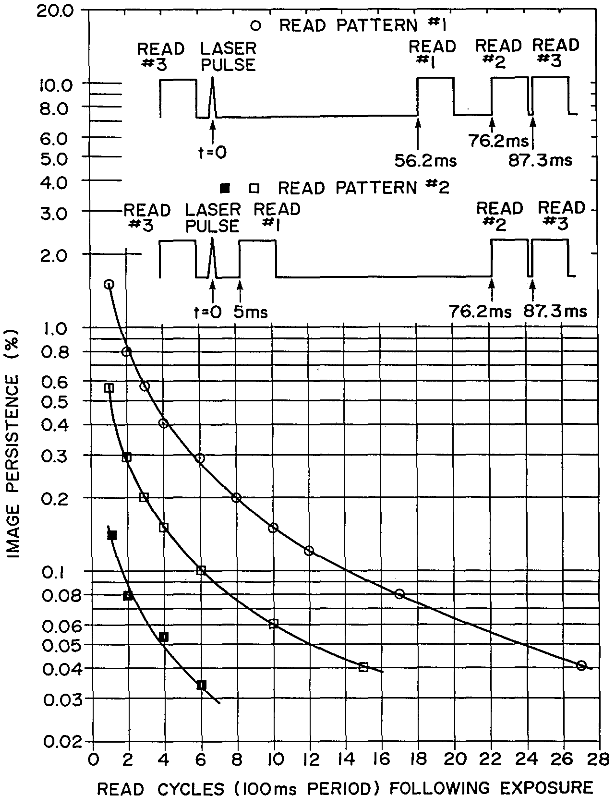

Fig. 3. Influence of read patterns on the image persistence of a TN-6132 IPDA detector (cooled to +2°C) for an interrupted 10-Hz exposure (open circles for read pattern No. 1, open squares for read pattern No. 2). The image persistence of an unintensified TN-6111 detector (cooled to 12°C) using read pattern No. 2 is shown for comparison (solid squares).

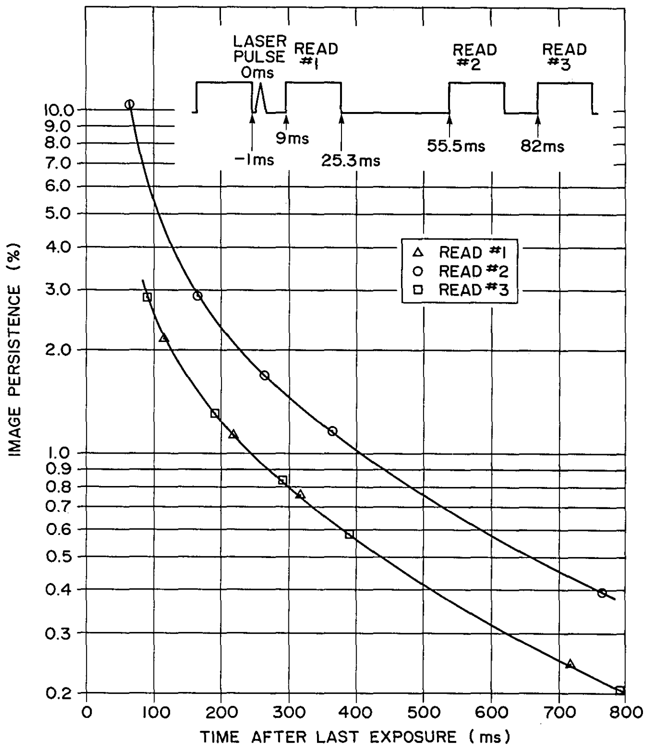

Fig. 4. Image persistence for a PI IRY-1024 IPDA following an interrupted 10-Hz exposure. Detector cooled to −7°C.

tor. This suggests that a failure to remove the accumulated charge on the diodes during readout of the array is not the major source of IPDA image persistence for the intensified detectors.

Similar results for the PI IRY-1024 (SN D128785) detector are shown in Fig. 4 where all three detector scans could now be digitized and stored. The diode array integrates the light from the IPDA phosphor and, if the accumulated charge on the diode array is completely removed during the detector scan, the observed signal represents $\int_{T_1}^{T_2} I_p\, dt$ where T_1 and T_2 are individual diode read times and I_p is the phosphor intensity. This interpretation is supported by the data in Fig. 4 where the total exposure time of an individual diode ($T_2 - T_1$) to the phosphor is approximately 26.5 ms for reads No. 1 and No. 3 and 46.5 ms for read No. 2. The relative intensities of the three curves (at a fixed time) are proportional to the exposure times. The effect of detector temperature on image persistence was not examined for the PI IRY-1024 (SN D128785).

Data supplied by Dr Y. Talmi[8] of Princeton Instruments for an IPDA with a comparable intensifier (a P-20 intensifier manufactured by Varo), and an unintensified array is shown in Table I. The initial diode scan occurred 17 ms after the xenon flash exposure, and subsequent scans at 51, 84, and 118 ms were digitized and expressed as a percentage of the initial scan.

With the unintensified diode array there is no appreciable image persistence thus supporting the conclusion, drawn from the data on the Tracor Northern detector, that the problem is not associated with incomplete removal of the accumulated signal from the diodes and further indicates that the diode array is not the source of the problem.

The image persistence shows a general tendency to increase with decreasing temperature. This is probably associated with a decreasing phosphor temperature resulting from conduction from the cooled diode array to the intensifier. The image persistence is at most a weak function of temperature between −13 and −25°C but exhibits a drop of ~35% as the temperature is raised to +25°C. This decrease in image persistence is gained at the cost of an increase in noise resulting from an increased diode array dark current.

To understand the effect of diode read pattern on image persistence we have constructed the integrated

Table I. Image Persistence: Comparison Between Unintensified and Intensified Detectors

Diode read time (ms)	Percentage image persistence: Unintensified array (25°C)	Intensified array (−25°C)	Intensified array (−20°C)	Intensified array (−13°C)	Intensified array (25°C)
51	0.28	4.11	4.06	3.79	2.58
84	0.04	1.23	1.20	1.27	0.76
118	0.02	0.52	0.57	0.67	0.39

IPDA intensity plots. A series of measurements were made where the delay in the diode read times was adjusted. For some experiments the laser was triggered during a detector read to obtain information at very short times (limited by the 10 μs read time for each individual diode of the TN-6132 detector). An example of these data for longer delay times is shown in Fig. 5 both for an interrupted 10-Hz laser exposure and following a single (isolated) laser exposure. An interrupted 10-Hz exposure refers to a succession of 2× ND:YAG laser pulses occurring at a 10-Hz frequency, imaged onto a detector, which was suddenly ceased. A single exposure refers to a solitary laser pulse, imaged onto a detector which was not previously exposed. The 10-Hz detector read pattern was maintained independent of laser exposure. The image persistence can still be detected 3 s after the interruption of a 10-Hz exposure, but following a single exposure it is much reduced and decays faster. This is to be expected since, for a single exposure, the effect due to the slowly decaying component of all the earlier pulses is absent.

We have used data such as those in Fig. 5 to construct the integrated detector intensity plots shown in Fig. 6. The solid curves are directly calculated from experimental data and, by definition, reach 100% at the time of the last observation. All of the contributions are summed to get the total intensity and then the integral $\int_0^T I_p\,dt$ is expressed as a fraction of this total. For the data shown in Fig. 5 we have calculated the quantity $\int_T^\infty I_p\,dt$ where T is the time of the last observation by assuming that the functional form of the decay (αt^{-n} where n is constant) continues to longer times. Thus the dotted curve in Fig. 6 includes an estimate of the integrated phosphor intensity for times t greater than 3 s for an interrupted 10-Hz exposure. For a single exposure the added intensity was not significant.

From Fig. 6 it can be seen that the intial fast rise in the integrated phospor intensity is followed by a much slower buildup. It can be seen that to minimize the signal remaining from all previous exposures, while still collecting most of the current exposure, the total time betwen read No. 3 of the previous cycle and read No. 1 of the current cycle should be minimized (to reduce diode integration time) as in read pattern No. 2 for the TN-6132 shown in Fig. 3. This reduces the observed image persistence in the first observation following the interruption of the exposure from 1.5% to 0.56%. The image persistence of the PI IRY-1024 was 2.2% (Fig. 4).

The TN-6132 integrated phosphor intensity curves (Fig. 6) show that the build up in signal is much slower for an interrupted 10-Hz exposure than for a single exposure. This implies that, in a typical CARS experiment, most of the image persistence results from exposures other than the previous one. This conclusion was confirmed by repeating the experiment in Fig. 2 for read pattern No. 2 and the TN-6132 detector but with a single exposure instead of an interrupted 10-Hz exposure. In the first cycle following the last exposure the image persistence was 0.17% for the single exposure

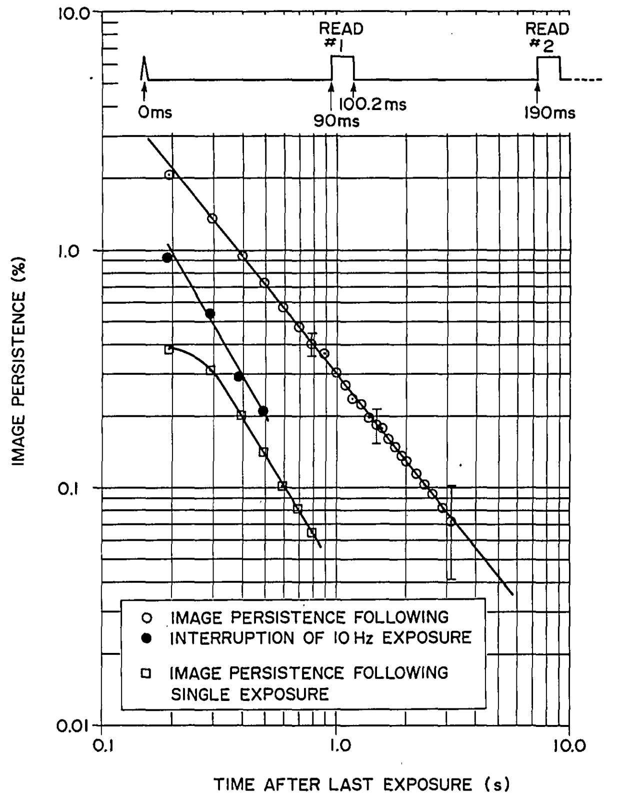

Fig. 5. Image persistence of a TN-6132 IPDA detector cooled to +2°C for an interrupted 10-Hz exposure (open circles) and a single exposure (open squares). The image persistence of a TN-6111 detector cooled to 12°C is shown for an interrupted 10-Hz exposure (solid circles).

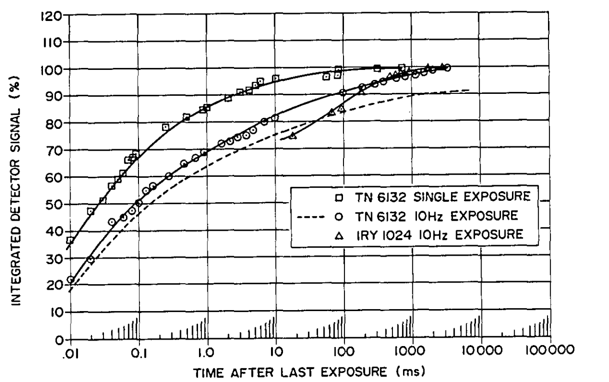

Fig. 6. Integrated phosphor intensities for interrupted 10-Hz and single exposures.

and 0.56% for the interrupted 10-Hz exposure, indicating that in the latter case at least 70% of the image persistence resulted from exposures other than the preceding one.

All of the measurements presented so far were for large initial signals near the upper limit of the A/D converters (~3000 counts for the TN-6132 and 12,000 counts for the PI IRY-1024). With a view of perhaps using the observed image persistence at the end of a 100-ms period to correct the data for the next cycle we investigated the effect of initial signal level on image persistence. The results for the TN-6132 are shown in Fig. 7 where read No. 1 is the last exposure and read No. 2 occurs in the next cycle (100-ms period). The image persistence, expressed as a fraction of the original signal, increases with decreasing initial signal level. (Similar behavior was observed with the PI IRY-1024 IPDA.) Thus weaker signals exhibit a greater image persistence. We had initially contemplated digitizing the detector cleansing scan at the end of each data acquisition period (e.g., read No. 3 in Fig. 4) to correct the next recorded scan (i.e. read No. 1 in the next 100-ms cycle) but the variation of image persistence with signal level makes implementing the necessary algorithm more difficult.

For CARS measurements in a turbulent environment, the signal will undergo large fluctuations and the image persistence will also be a function of the intensity history of several previous CARS pulses rather than the single preceding pulse. This further complicates the implementation of an algorithm to correct for image persistence.

Our observations on image persistence are based on measurements on two separate Tracor Northern 6000 series detector systems and two Princeton Instruments IRY-1024 systems, all incorporating P-20-based intensifiers from two different intensifier manufacturers. Talmi[8] has observed behavior similar to that shown in Table I for several additional detectors incorporating P-20-based intensifiers.

In addition to these measurements Barton and Richer[12] have investigated the image persistence of an EGG/PARC 1420B IPDA incorporating a P-20-based intensifier. They interrupted a 10-Hz exposure and the IPDA was read once per 100-ms period beginning 1.5 ms after the laser pulse. They followed the decay for 1.4 s (14 scans 100 ms apart) and found that only 74% of the total signal in all 14 scans occurred in the first scan. This experiment provides additional evidence that the high image persistence is generic to all P-20-based IPDA detectors.

We have evaluated[10] a prototype Princeton Instruments detector with a rare earth phosphor-based intensifier using essentially the same IPDA read pattern as shown in Fig. 4. The image persistence for the first pulse (read No. 1) following the initial scan of the last exposure was 0.06%, which is ~40 times less than for the corresponding P-20-based system. The detector sensitivity at 500 nm was 4.5 photons/count, which is comparable to that of the P-20 phosphor-based detectors we have measured (1.7, 3.4, 2.9, and 3.5 photons/count). This detector exhibited none of the nonlinearity we have found with the P-20-based systems.

The image persistence will be a function of the total detector read time since this time, plus the necessary delay between the laser pulse and the start of the read cycle, is the total detector integration time. For example, a detector with a 4-ms total read time (instead of 16 ms) would have reduced the image persistence for the read pattern in Fig. 4 (with a 9-ms delay) by almost a factor of 2.

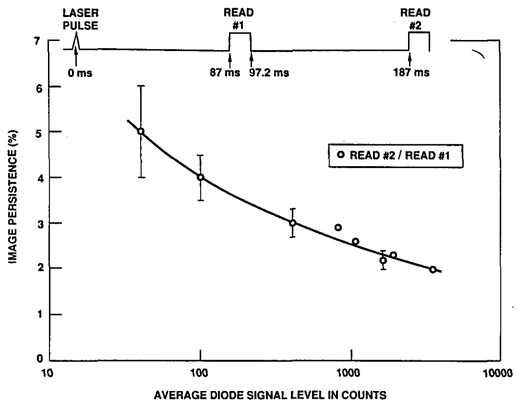

Fig. 7. Interrupted 10-Hz image persistence vs incident signal level for a TN-6132 IPDA detector cooled to +2°C.

IV. Summary and Conclusions

From analysis of the behavior of several P-20 phosphor-based intensified self-scanning photodiode arrays (IPDA) we conclude that these detectors suffer from a greater image persistence (lag) than has generally been realized. For a typical 10-Hz CARS experiment the image persistence is 0.5–2.0% of the average signal level, the bulk of which results from pulses other than the preceding one. This will result in CARS temperature measurements in turbulent combustion being biased to lower temperatures. A more detailed examination of temperature errors caused by image persistence is presented in an accompanying publication in this issue.

The P-20 IPDA detectors also exhibit a fall off in sensitivity at lower output signals that can be described as logarithmic with output signal or, alternatively, as an IPDA output in counts that varies as greater than the first power of light intensity. Applying a correction to CARS data for this nonlinearity results in a best-fit temperature that is 40–90-K hotter at a flame temperature of 1600 K.

A prototype IPDA incorporating a rare earth phosphor was examined and found to be clearly superior for CARS spectroscopy. The image persistence was ~40 times less than for the corresponding P-20 phosphor system and the detector sensitivity was constant with signal level. We are currently acquiring an IPDA with this rare earth phosphor and a faster read time (4 ms for 1024 elements) that should be much better suited to turbulent combustion measurements than the existing P-20 IPDA detectors.

References

1. R. K. Chang and M. B. Long, "Optical Multichannel Detection," in *Light Scattering in Solids II*, M. Cardona and G. Guntherodt, Eds. (Springer-Verlag, Berlin, 1982), pp. 179–205.
2. Y. Talmi and R. W. Simpson, "Self-Scanned Photodiode Array: A Multichannel Spectrometric Detector," Appl. Opt. **19**, 1401–1424 (1980).
3. L. P. Goss, D. D. Trump, B. G. MacDonald, and G. L. Switzer, "10-Hz Coherent Anti-Stokes Raman Spectroscopy Apparatus for Turbulent Combustion Studies," Rev. Sci. Instrum. **54**, 563–571 (1983).

4. D. R. Snelling, R. A. Sawchuk, and R. E. Mueller, "Single Pulse CARS Noise: A Comparison Between Single-Mode and Multimode Pump Lasers," Appl. Opt. **24**, 2771–2778 (1985).
5. D. R. Snelling, G. J. Smallwood, R. A. Sawchuk, and T. Parameswaran, "Precision of Multiplex CARS Temperatures using both Single-Mode and Multimode Pump Lasers," Appl. Opt. **26**, 99–110 (1987).
6. D. R. Snelling, A. Sawchuk, and G. J. Smallwood, "Multichannel Light Detectors and Their Use for CARS Spectroscopy," Appl. Opt. **23**, 4083–4089 (1984).
7. R. R. Antcliff, M. E. Hillard, and O. Jarrett, Jr., "Intensified Silicon Photodiode Array Detector Linearity: Application to Coherent Anti-Stokes Raman Spectroscopy," Appl. Opt. **23**, 2369–2375 (1984).
8. Y. Talmi, Princeton Instruments, Trenton, NJ, private communication.
9. S. Kroll, M. Alden, P. -E. Bengtsson and C. Lofstrom, "An Evaluation of Precision and Systematic Errors in Vibrational CARS Thermometry," J. Appl. Phys. B, in press.
10. D. R. Snelling, National Research Council of Canada, Div. of Mechanical Engineering, Ottawa, Ontario, Canada, unpublished results.
11. D. R. Snelling, G. J. Smallwood, and T. Parameswaran, "Effect of Detector Nonlinearity and Image Persistence on CARS Derived Temperatures," Appl. Opt. **28**, 3233–3241 (1989).
12. S. Barton and G. Richer, Defence Research Establishment Valcartier, Quebec, Canada; private communication.

NASA *continued from page 3225*

restricted somewhat so that the dependence of the shift on frequency does not, itself, result in decorrelation. (However, a correction for this dependence could presumably be made in the synthetic spectrum.)

This work was done by Reinhard Beer and Robert H. Norton, Jr., of Caltech for NASA's Jet Propulsion Laboratory. Refer to NPO-17306.

Phase modulation gas correlation spectroscopy

Electrooptic phase modulation gas correlation spectroscopy has been demonstrated in laboratory tests to be a promising candidate technique for remote sensing of gases, temperatures, and wind velocities in the atmosphere. In this technique radiation emitted by the sample atmosphere is passed through an electrooptic phase modulator, and the modulated and unmodulated versions of the spectrum are alternately passed through a reference absorption cell containing the gas to be detected. The radiation emerging from the reference cell is bandpass filtered and detected. The correlation signal is the difference in intensity between the phase modulated and unmodulated detected signals. The phase modulation redistributes the emission spectrum into upper and lower sidebands displaced from the original spectral lines by integral multiples of the modulating frequency. Emission or absorption lines in the modulated sample spectrum that correlate with absorption spectral lines of the gas in the reference cell alter the power transmitted to the detector. Thus, the measurement is most sensitive to the spectrum in the input radiation corresponding to the species contained in the reference cell.

The laboratory prototype system shown in Fig. 9 has been used to measure part of the infrared spectrum of N_2O. Blackbody radiation from a glow bar at a temperature of 1000 K is chopped mechanically at a rate of 500 Hz and passes through a 1-cm thick cell containing the N_2O sample gas. The radiation, which now contains an N_2O absorption spectrum, passes through an electrooptic phase modulator and through a 1-cm thick reference cell containing N_2O. The modulator, a CdTe crystal, is activated and deactivated by turning a 15-W 100-MHz modulating signal on and off at a repetition rate of 10 kHz. A lock-in amplifier synchronized to the 10-kHz signal processes the detector output to obtain the correlation signal. Another lock-in amplifier synchronized to the mechanical chopper processes the detector output to obtain a measure of the total radiant energy transmitted through the system.

The system was tested at various pressures of N_2O in the sample and reference cells from 0 to 10 Torr (0 to 1.3 kPa). The measurements showed that as the pressure in the sample cell rises (at a given fixed pressure in the reference cell), the correlation signal first increases, then levels off to a maximum, then decreases. The experimental and theoretical correlation curves were in excellent agreement.

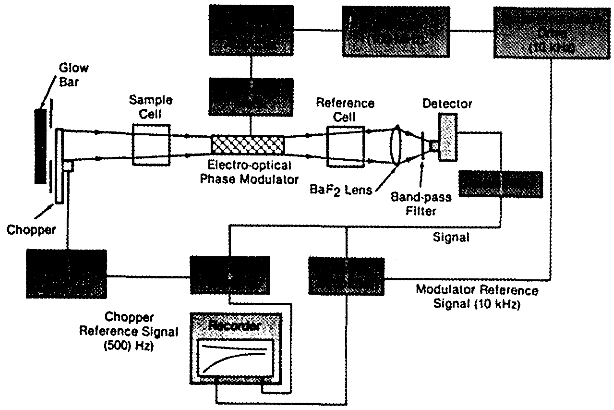

Fig. 9. This laboratory prototype system was used to demonstrate electrooptic phase modulation gas correlation spectroscopy.

This work was done by David M. Rider, John T. Schofield, Jack S. Margolis, and Daniel J. McCleese of Caltech for NASA's Jet Propulsion Laboratory. Refer to NPO-17013.

Thermal wave microscope

A computer controlled thermal wave microscope has been developed to investigate III–V compound semiconductor devices and materials. Thermal wave microscopy is a nondestructive technique that can provide information on subsurface thermal features of solid samples. Furthermore, because this is a subsurface technique, 3-D imaging is also possible. Thermal wave imaging is performed with a modified scanning electron microscope (see Fig. 10). An intensity modulated electron beam generates thermal waves in the specimen. The modulation frequency is typically in the range of 0.1–10 MHz.

The thermal waves generated by the electron beam are critically damped, but they interact with thermal features in the specimen. The thermal waves are not detected directly. Instead, the acoustic waves generated by the thermal waves are detected by an acoustic transducer glued to the sample. The transducer signal is amplified and fed to a lock-in amplifier before undergoing analog-to-digital conversion. The image is built up point by point as the electron beam is indexed through a raster of points under the control of the computer. The software that controls the scanning electron microscope and handles the image data was written in FORTRAN 77. Thermal wave microscopy is limited by low signal levels, extremes in signal contrast, and poor edge definition. However, once the image data are in the computer, various digital techniques can be used to enhance features of interest in the image. The resulting images can be fed back to the scanning electron microscope for display or can be stored on a magnetic disk.

continued on page 3254